

# The Plasma Wave Instrument On Board the AMPTE IRM Satellite

B. HÄUSLER, R. R. ANDERSON, D. A. GURNETT, H. C. KOONS, R. H. HOLZWORTH, O. H. BAUER, R. TREUMANN, K. GNAIGER, D. ODEM, W. B. HARBRIDGE, AND F. EBERL

**Abstract**—The AMPTE IRM plasma wave instrumentation is designed to provide basic information on the plasma wave activity in the magnetosphere/solar-wind environment and inside the artificial plasma clouds which will be created in space. The instruments use one long electric dipole antenna and two magnetic search coil sensors in order to cover frequency ranges from dc to 5.6 MHz for the electric measurements and from about 30 Hz to 1.5 MHz for the magnetic measurements. A set of spectrum analyzers along with a fast memory and an analog wide-band system are used to determine wave intensities and to identify wave modes.

## I. INTRODUCTION

THE PLASMA wave instrumentation on board the IRM is devoted to the measurement of dc electric fields, electrostatic and electromagnetic waves in the magnetosphere/solar-wind environment, and inside the artificial plasma clouds which will be created in space.

The electric wave measurement utilizes a long (~47 m tip-to-top) antenna to measure electric fields from dc to ~5.6 MHz, and two boom-mounted search-coil magnetometers to measure magnetic fields from 30 Hz to ~1.5 MHz. Spectrum analyzers, sweep-frequency receivers are used to detect signals at ELF frequencies and above. The available time resolution for complete frequency sweeps in the highest bit rate mode is 1 s, well suited for the recording of boundary-layer phenomena. In addition, the instruments provide the possibility of the storage of wave data with a very high time resolution of 32 ms and the receiving/transmission of wide-band analog data with a bandwidth of dc to 10 kHz.

The circuitry that measures the difference in antenna potential ( $V_{DIFF}$ ) up to 32 times/s allows the determination of the dc electric field and ULF waves up to 16 Hz in the dense

plasma regimes in the release clouds and in the plasmasphere. Meaningful dc electric-field measurements are difficult to make in the solar wind and low-density regions of the magnetosphere [1], [2]. The exact plasma number density and temperature where our dc measurements are reliable will have to be determined in orbit.

A survey of important parameters of the instruments is given in Table I and the location of the instruments in the satellite is shown in the spacecraft description document [3].

Special care has been given to protect radiation-sensitive parts such as CMOS IC's with the appropriate amount of shielding material (~1.2 g/cm<sup>2</sup> of aluminum equivalent to a yearly dose of ~10<sup>4</sup>-rads Si). Of great importance were also the efforts undertaken at the instrument and spacecraft level to guarantee an electromagnetically clean environment. These are described in [3].

## II. SCIENTIFIC AIMS

The instrument set has been designed to provide high time resolution measurements with narrow-band as well as broad-band frequency resolution. It is therefore well suited to perform a survey of natural phenomena, such as boundary layers, bow shock, magnetopause, and plasma sheet. In particular, this investigation should greatly benefit from the existence of simultaneously performed wave measurements on board the UK satellite.

Important frequency ranges which will be covered are the electron plasma frequency, electron-cyclotron frequency, lower hybrid frequency, ion-cyclotron frequencies, and the high-frequency range of terrestrial kilometric radiation and interplanetary type-III emissions (for a review see [4]–[6]). Waves near the electron-cyclotron frequency and electron plasma frequency are expected to occur in regimes where anisotropic electron distributions as well as electron beams prevail (upstream bow shock, inner magnetosphere, plasma sheet).

Waves near the ion plasma frequency and lower hybrid waves are expected to occur in regimes where ion beams or two-stream conditions dominate (upstream bow shock, foot region, magnetopause, neutral sheet) (e.g., [7]–[9]). High-frequency electromagnetic waves originate in the solar wind or corona, possibly also upstream of the bow shock, inner magnetosphere, and on auroral field lines (e.g., [10]–[12]).

During the plasma cloud releases, very fast changes of plasma parameters and transitions between different plasma states are expected to occur. This should lead to variations in the dc electric field and to the generation of a variety of different

Manuscript received October 17, 1984. University of Iowa participation was supported under Contracts N0014-82-K-0183 and N00014-76-C-0016. Aerospace Corporation participation was supported in part by the Office of Naval Research and in part by the U.S. Air Force System Command's Space Division under Contract F04701-84-C-0085. Research at the University of Washington was supported by the Office of Naval Research under Contract N00014-84-K-0160.

B. Häusler, O. H. Bauer, R. Treumann, and F. Eberl are with the Max-Planck-Institut für Physik und Astrophysik, Institute für extraterrestrische Physik, 8046 Garching, Germany.

R. R. Anderson, D. A. Gurnett, and D. Odem are with the Department of Physics and Astronomy, University of Iowa, Iowa City, IA 52242.

H. C. Koons and W. B. Harbridge are with the Space Sciences Laboratory, Aerospace Corporation, Los Angeles, CA 90009.

R. H. Holzworth is with the Space Sciences Division, University of Washington, Seattle, WA 98185.

K. Gnaiger is with Kurt Gnaiger Mikroelektronik, 8046 Garching, Germany.

TABLE I  
IMPORTANT PARAMETERS OF THE VARIOUS INSTRUMENTS BELONGING TO THE  
AMPTe IRM PLASMA WAVE EXPERIMENT

Unit	Institute	Frequency Range	Steps / Channel	Frequency Resolution Bandwidth	Power (W)	Mass (kg)
VLF/MF SFR 1	Aerospace	275 - 2525 Hz	32 st	100 Hz	4.7	4.6
VLF/MF SFR 2		900 - 9900 Hz	32 st	300 Hz		
VLF/MF SFR 3		9000 - 99 kHz	32 st	3 kHz		
E-field-preamp.						
VLF-search coil + boom + preamp.	MPE	30 Hz - 60 kHz			0.2	1.1
E-field antenna mechanism + control-unit	MPE U. of Iowa				10.0	3.8
E-field preamps	U. of Iowa	DC - 6 MHz				
ELF/MF spectrum analyzer	U. of Iowa			±/-19% low frequency	2.5	4.7
peak		31 Hz - 178 kHz	16 ch	±/-11% high frequency		
average		31 Hz - 178 kHz	16 ch			
shock		31 Hz - 178 kHz	16 ch			
V-diff		DC - 30 Hz	1 ch			
High-frequency receiver	U. of Iowa	100.8 kHz - 5.6 MHz	42 st	10 kHz	2.0	
Wide-band analog receiver	U. of Iowa	DC - 10 kHz	1 ch	analogue modulation	0.9	
HF spectrum analyzer	MPE	28 kHz - 1.54 MHz	64 st	24 kHz	1.8	2.1
HF-search coil + boom + preamp.	MPE	10 kHz - 2 MHz			0.2	0.9
Data-control unit	MPE				0.8	4.3
Shock memory		131 k byte	16 ch	minimum sampl. period for one spectra 32 msec	0.2	
Mux					0.8	1.1
Total Mass (kg)						22.6

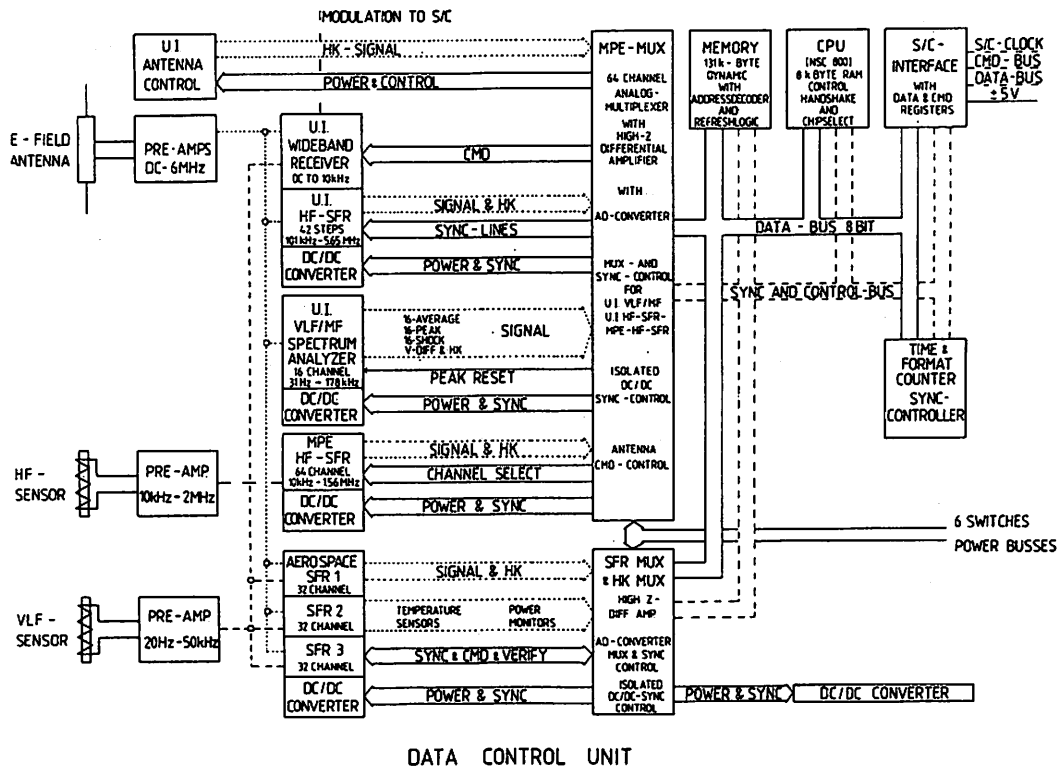


Fig. 1. Block diagram of the plasma wave instrument.

plasma waves, ranging from the MHD regime to the kinetic electron plasma wave regime [13]. A detailed description of the scientific goals of the release experiments is given elsewhere [14]-[17].

### III. DIGITAL CONTROL OF PLASMA WAVE INSTRUMENTS

Fig. 1 shows a block diagram of the plasma wave instrument set. In its left section the electric antenna, magnetic sensors, and analogue instruments are shown; the right section shows the digital control unit (DCU) of the instrument set.

#### A. Digital Control Unit (DCU)

The plasma wave DCU provided by the Max-Planck-Institut controls the complete plasma wave instrument set. It operates in synchronism with the spacecraft clock. The main tasks of the DCU are to:

- 1) provide one serial data and command interface from the individual plasma wave instruments to the spacecraft;
- 2) a/d convert all data via high-impedance differential inputs with 8-bit resolution;

- 3) provide isolated dc/dc synchronization pulses; and
- 4) control the fast 131-kbyte plasma wave memory (dynamic).

The heart of the DCU is an NSC-800/883 B CPU. The program operates from two (2K × 8) byte RAM and two (2K × 8) byte ROM memories.

In order to protect the plasma wave instrument set against failures that might be caused by radiation damage, the DCU is equipped with a redundant ROM/RAM set. The active set can be selected by telecommand.

Power consumption of the DCU is 1.6 W at +28-V supply voltage.

### B. Memory

The plasma wave instrument package provides the possibility of storing wave data with a very high time resolution in a memory. The memory provided by the Max-Planck-Institut is of the "continuous cycle" type. When activated, data will be continuously stored unless the WRITE mode is inhibited by command. Its storage capability is 131 072 byte, and it consists of 16 8-kbyte NMOS RAM IC's (Siemens, HYB 4164). The ELF/MF spectrum analyzer (see Section IV-B) provides 16 special fast outputs ("shock" channels) which can be sampled with a selectable time resolution of 32, 64, 128, and 256 ms. In the fastest mode data can be stored for a time period of approximately 4 min. The memory is also used to store magnetometer data needed for attitude determination during time periods where there is no ground station telemetry coverage. The refresh and control logic of the memory is done by the plasma wave DCU. The memory board is operated at +5 V, and its power consumption is  $\leq 0.2$  W.

## IV. dc/ac ELECTRIC FIELD

### A. Antenna

The electric antenna which is provided by the Max-Planck-Institut is an extendible beryllium-copper dipole element with a tip-to-tip length of 47.42 m. The diameter of the element is typically 5 mm. The extension/retraction mechanism is very similar to the one flown by the University of Iowa on the Hawkeye spacecraft. The antenna is covered with an insulating layer out to a distance of 15.55 m on each half of the dipole. The total mass of the unit is 1205 g.

A complete antenna extension lasts approximately 35 min. Dynamical stability considerations and other mechanical aspects concerning flexible antenna elements on board a rotating spacecraft with ejectable canisters are treated in [18] and [19].

The antenna control logic is supplied by the University of Iowa.

### B. ELF/MF Spectrum Analyzer (dc-178 Hz)

The plasma wave instrument set contains six preamplifiers for detecting electric signals.

Two low-frequency preamplifiers with a gain of 4.0 are driven single-ended from each antenna element, and feed the 16-channel ELF/MF spectrum analyzer (this section) and also the wide-band receiver (Section IV-E). Further, two dc pre-

amplifiers having a gain of 0.25, also driven single-ended from each antenna element, are used for the antenna potential difference ( $V_{DIFF}$ ) and the antenna potential measurements. The outputs operate over the frequency range of 0.1-20 Hz.

The ELF/MF spectrum analyzer provided by the University of Iowa is a spare unit of the Helios project. Its main elements are 1) a differential amplifier, 2) a 16-channel spectrum analyzer, 3) an antenna potential monitor, and 4) a power supply. This analyzer provides relatively coarse frequency coverage and rapid temporal resolution with essentially continuous coverage of all frequencies from 20 Hz to 200 kHz and all times by using peak detectors. The 16 center frequencies are spaced logarithmically (31.1 Hz, 56.2 Hz, 100 Hz, 178 Hz, 311 Hz, ..., 178 kHz) and have bandwidths of approximately  $\pm 19$  percent for channels 1-8 and  $\pm 11$  percent for channels 9-16. The detector and log compressor in each channel will rectify and logarithmically compress signals from the filter and produce an output voltage proportional to the logarithm of the noise intensity in each filter channel. The dynamic range of the log compressors is about 100 dB. The log compressor output is used to provide three outputs for each channel: 1) a peak output, 2) an average output, and 3) a short time-constant shock output.

The average output provides an RC output with either 1) a time constant  $\tau$  which depends on the bit rate, or 2) a forced short time constant  $\tau_s$ . The instrument is usually operated in the "forced short-time-constant" mode which corresponds to  $\tau_s = 50$  ms for channels 3-16. The sixteen peak and average outputs are sampled within 32 ms. The sampling frequency is proportional to the spacecraft bit rate (1 Hz at 8 kbit/s, 0.5 Hz at 4 kbit/s, etc.). The peak output measures the peak signal over the sampling period. The fast shock outputs provide short-time-constant voltages to the shock memory (see Section III-B).

The antenna potential monitor measures the average potential  $V_{AVG}$ , which is the average of both antenna potentials against payload potential, and the potential difference between both antennas  $V_{DIFF}$ . The frequency range of the  $V_{DIFF}$  measurements is from 0.1 to 20 Hz which allows for both dc and ELF measurements since the spacecraft spin rate is  $\sim 0.25$  Hz. The dynamic range of the  $V_{DIFF}$  measurements is controlled by command to be either  $\pm 8.4$ ,  $\pm 2.1$ , 0.52, or 0.131 V. Taking into account an effective antenna length of 39.25 m for dc measurements and the 8-bit A/D conversion, the minimum sensitivity levels corresponding to the four gain states are 1.66, 0.416, 0.104, and 0.026 mV/m, respectively. The dynamic range of the  $V_{AVG}$  circuitry is from +40.0 to -40.0 V. The sampling period of  $V_{DIFF}$  and  $V_{AVG}$  is proportional to the bit rate of the spacecraft. For the highest bit rate (8 kbit/s) the sampling period is 32 ms and 2 s, respectively.

The unit draws 90 mA—corresponding to  $\sim 2.5$  W at +28 V. The dc-dc converter is synchronized by the DCU with 43.7 kHz which is one third of the spacecraft clock frequency (131.072 kHz).

### C. VLF/MF Stepped-Frequency Receiver (275 Hz-99 kHz)

The stepped-frequency receiver (SFR) can be connected to either the VLF search coil (see Section V) for magnetic mea-

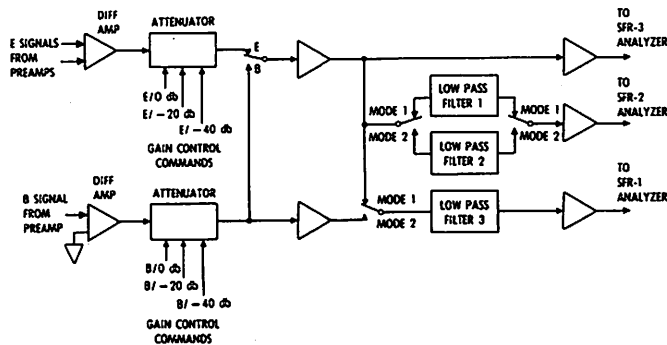


Fig. 2. VLF/MF stepped-frequency receiver input and mode switching possibilities. The three analyzers cover a frequency range from 275 Hz to 99 kHz.

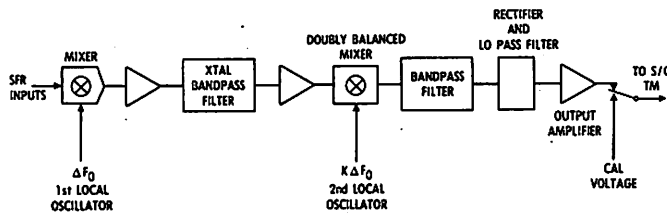


Fig. 3. Block diagram of one stepped-frequency analyzer.

measurements or the long plasma wave antenna for electric field measurements.

The block diagram of the SFR which is provided by the Aerospace Corporation is shown in Fig. 2. The receiver has three separate 32-step spectrum analyzers with fully synthesized local oscillators controlled by an internal program. The three analyzers may be operated in parallel or separately and switched to either the electric or magnetic antenna by command. Fig. 3 shows the block diagram of one stepped-frequency receiver.

The SFR is normally operated in mode 1 and covers the following frequency bands: 275–2525 Hz (SFR-1), 900–9900 Hz (SFR-2), and 9–99 kHz (SFR-3). In mode 2 the SFR simultaneously analyzes signals from the magnetic antenna using SFR-1 and from the electric antenna using SFR-2 over the frequency range from 275 to 2525 Hz. In mode 2, SFR-3 is tuned to the electric antenna and analyzes the band from 9 to 99 kHz. The corresponding channel bandwidths are: 100 Hz, 300 Hz, and 3 kHz, respectively.

The instrument can be commanded to one of three dynamic ranges. The entire dynamic range of the instrument is 100 dB. The minimum detectable signal level is set to 10  $\mu$ V.

The automatic stepping rate depends on the spacecraft bit rate. In the highest bit-rate mode (8 kbit/s), the stepping rate is 32 steps/s. The instrument can also be commanded to remain continuously on any of the 32 steps.

The SFR also has its own power supply. It draws 168 mA at +28 V—equivalent to a power consumption of 4.7 W—when in its full operating mode.

#### D. HF Stepped-Frequency Receiver (100 kHz–5.6 MHz)

The high-frequency preamplifier, also provided by the University of Iowa, has a differential input amplifier and a gain of approximately 4.0. The output of the high-frequency preamplifier provides signals to the high-frequency receiver which

covers the frequency range from 100 kHz to 5.6 MHz in 42 discrete steps with a bandwidth of about 10 kHz. In the highest bit rate, the entire band is covered in 2 s. The frequency at each step is determined by six clock lines. The 10-kHz band-limited signal at each frequency step is fed into a log compressor which has a dynamic range of  $\sim$ 100 dB. A block diagram of the receiver is shown in Fig. 4.

The power supply converts the +28-V dc line from the spacecraft into regulated voltages for the wideband receiver (Section IV-E) and the high-frequency receiver. It draws 105 mA—equivalent to a power consumption of 2.9 W—and is also synchronized with 43.7 kHz, one third of the spacecraft clock frequency (131.072 kHz).

#### E. Wide-Band Analog Receiver (dc–20 kHz)

The purpose of this wide-band receiver is to condition broadband signals for direct transmission to the ground. The receiver is provided by the University of Iowa. It shares the electric preamplifiers with the VLF/MF spectrum analyzer. Its input can also be selected by command to the magnetic antenna (see Section V). Two wide-band channels are transmitted to the ground. An automatic gain control receiver covering the frequency range from 650 Hz to 10 kHz provides the baseband channel. The second channel is a frequency-modulated subcarrier at 13.5 kHz which contains the dc compressor output for the frequency range 5 Hz to 1 kHz.

AGC values and dc compressor signals are being transmitted in the PCM frame with a sample period of 0.5 s (highest bit rate). The wide-band signal modulates directly the S-band carrier frequency. It is added to the filtered PCM subcarrier signal (131072 Hz) in the main spacecraft electronics.

The receiver is contained in the HF stepped-frequency receiver box (Section IV-D) and shares its power supply.

### V. ac MAGNETIC FIELD

#### A. Sensors

Two search-coil antennas (VLF and HF) were installed on board the IRM spacecraft. They were mounted on rigid booms approximately 90 cm above the instrumentation plane (see [3, Fig. 1]). Each antenna covers a specific frequency range: 20 Hz–60 kHz and 10 kHz–2 MHz.

The VLF antenna is  $\sim$ 26 cm long, has a cross section of 1 cm<sup>2</sup>, and has a  $\mu$ -metal multilayer core. The HF antenna is of the same dimension but uses a ferrite core. The VLF antenna is connected to a preamplifier using active flux feedback technique. It is, therefore, possible to achieve a flat transfer function across a wide frequency range.

The noise levels of the preamplifier/sensor combination are:

$$\begin{aligned} \text{at: } 30 \text{ Hz} & \quad \sim 4 \times 10^{-1} \frac{\text{pT}}{\sqrt{\text{Hz}}} \\ 300 \text{ Hz} & \quad \sim 10^{-2} \frac{\text{pT}}{\sqrt{\text{Hz}}} \quad \left( \sim 7 \times 10^{-2} \frac{\text{pT}}{\sqrt{\text{Hz}}} \right) \\ 3 \text{ kHz} & \quad \sim 10^{-3} \frac{\text{pT}}{\sqrt{\text{Hz}}} \quad \left( \sim 10^{-2} \frac{\text{pT}}{\sqrt{\text{Hz}}} \right) \\ 30 \text{ kHz} & \quad \sim 10^{-2} \frac{\text{pT}}{\sqrt{\text{Hz}}} \quad \left( \sim 10^{-2} \frac{\text{pT}}{\sqrt{\text{Hz}}} \right). \end{aligned}$$

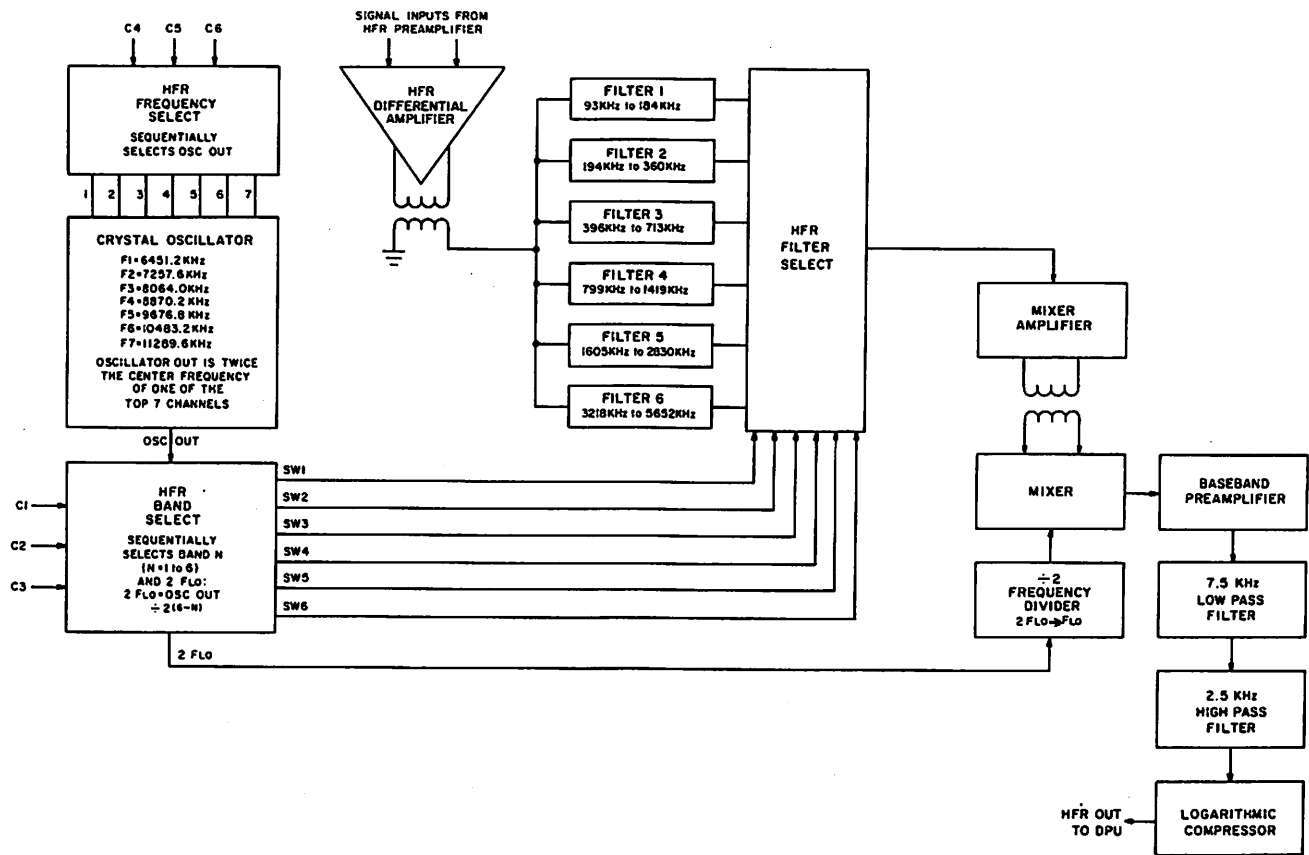


Fig. 4. Block diagram of the high-frequency receiver for detection of electric signals in the frequency range of 100 kHz–5.65 MHz.

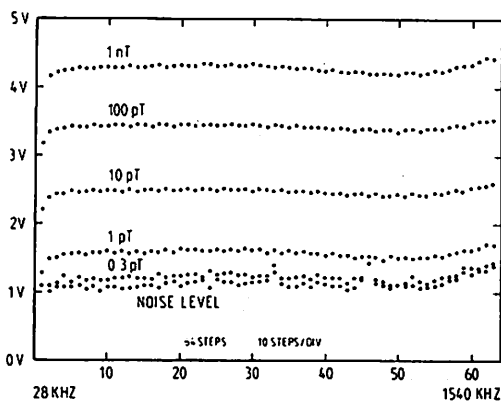


Fig. 5. Calibration of high-frequency stepped-frequency receiver and magnetic sensor. The unit covers a frequency range of 28 kHz–1.54 MHz.

The values given in parenthesis are based on measurements in orbit. They reflect the effective noise due to the spacecraft environment.

The magnetic HF preamplifier is driven single-ended by the HF search coil. The transfer function is also flat across a wide frequency range. The unit offers a dynamic range of ~80 db measured in a 25-kHz bandwidth (see Fig. 5).

**B. Receivers (20 Hz–1.56 MHz)**

The signal of the VLF search coil can be linked by command to the VLF/MF stepped-frequency receiver (Section IV-D) and to the wide-band analogue receiver (Section IV-E). The

plasma wave DCU commanding capabilities allow the input of both receivers to be switched separately between the E and B antenna or in-phase/out-of-phase between both units (see also Figs. 1 and 2).

The signal of the HF search coil preamplifier output feeds a separate 64-channel stepped-frequency receiver. Its block diagram is shown in Fig. 6. It continuously covers a frequency range of 28–1540 kHz (center frequency). The channel bandwidth is 24 kHz, its input sensitivity is 0.3 μV, and it has a dynamic range of ~110 dB. The output signal is logarithmically compressed. The stepping rate is synchronized with the spacecraft bit rate. A full frequency coverage (64 channels) takes 4 s in the high-bit-rate mode.

The start frequency of the sequencer can be commanded to any one of the 64 channels. Another command allows the instrument to stay continuously at one channel. If channel number 0 is commanded, the injected VCO signal is identical to the IF frequency; it can be used as a calibration signal for the receiver.

The stepped-frequency receiver and the magnetic sensors are supplied by the Max-Planck-Institut.

**VI. IN-FLIGHT OPERATION**

The AMPTE IRM plasma wave instruments were turned on three days after launch, shortly before the extension of the long electric antenna. The antenna was extended to its full length within 1 h, including short interruptions at 2 and 45 m to verify proper functioning. The instruments are being con-

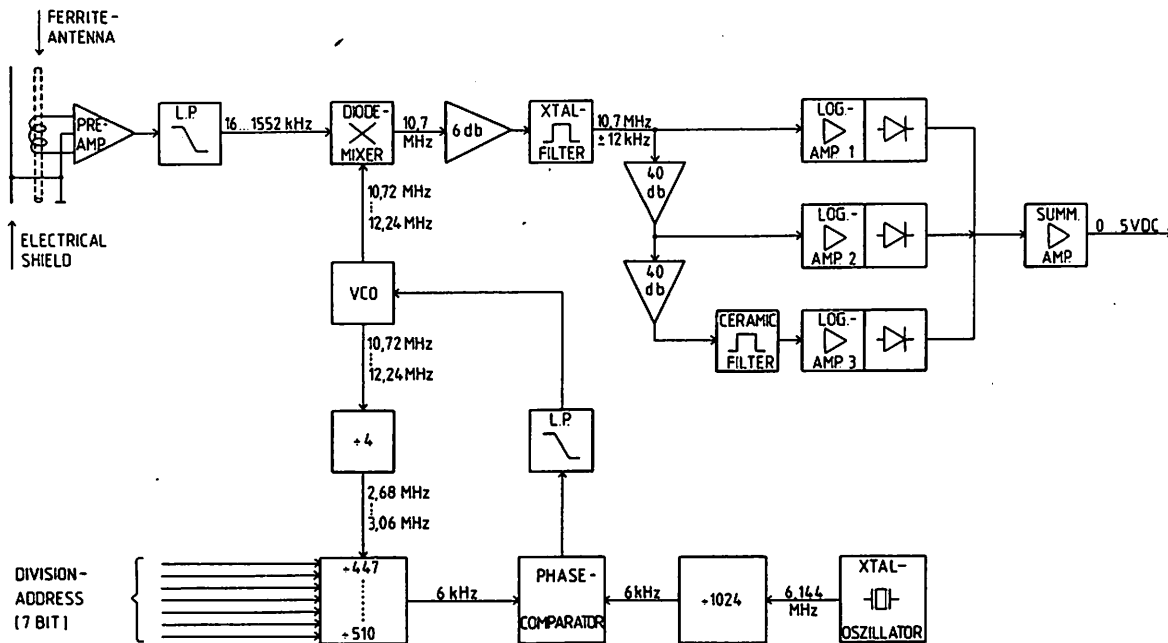


Fig. 6. Block diagram of the stepped high-frequency receiver for magnetic fluctuations (28 kHz-1.56 MHz).

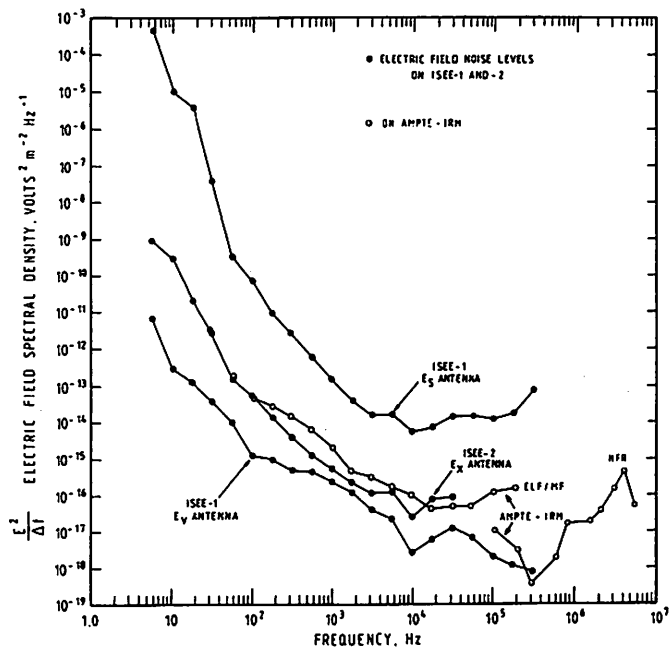


Fig. 7. Comparison of in-flight noise levels measured with the electric antenna of AMPTE IRM with plasma wave instruments of other spacecraft. ISEE-1 and -2 data are taken from [20].

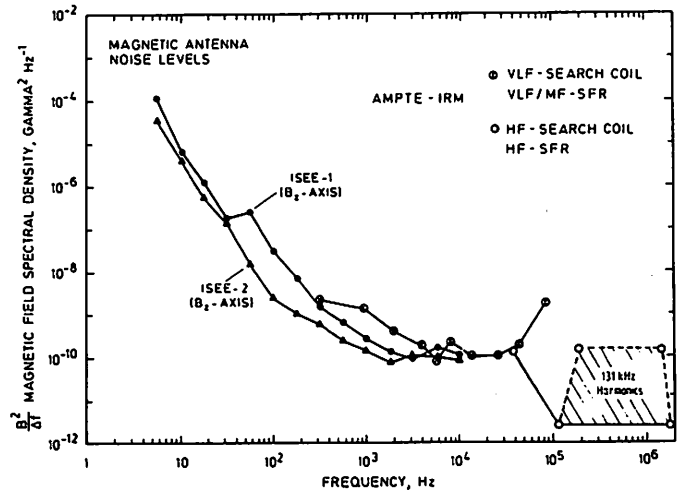


Fig. 8. Comparison of in-flight noise levels measured with the magnetic sensors of AMPTE IRM with instruments of other spacecraft. ISEE-1 and -2 data are taken from [20].

tinuously operated since then during time periods where telemetry ground-station coverage is provided.

The wide-band system was activated for time periods of approximately 6 h before and after a release window.

Representative noise levels for the electric and magnetic measurements in comparison with other spacecraft such as ISEE-1 and ISEE-2 are shown in Figs. 7 and 8 [20].

ACKNOWLEDGMENT

We wish to express our appreciation to our many colleagues who participated in the development, testing, and integration of this instrumentation. In particular, we acknowledge the

efforts of R. D. Anderson, M. Bailey, D. Kirchner, and J. Knowlton (University of Iowa), D. Katsuda (Aerospace Corp.), and P. Genzel (ESTEC). The authors are also indebted to F. X. Sené (CRPE, Siemel) and R. Kramer (Fairchild Space and Electronics Corp.) for their contribution to the design and construction of the search coil antennas and the electric wave antenna mechanism.

REFERENCES

- [1] J. P. Heppner, E. A. Bielecki, T. L. Aggson, and N. C. Maynard, "Instrumentation for DC and low-frequency electric field measurements on ISEE-1," *IEEE Trans. Geosci. Electron.*, vol. GE-16, no. 3, p. 253, 1978.
- [2] A. Pedersen, C. A. Catell, C.-G. Fälthammar, V. Formisano, P.-A. Lindqvist, F. Mozer, and R. Torbert, "Quasistatic electric field measurements with spherical double probes on the GEOS and ISEE satellites," *Space Sci. Rev.*, vol. 37, p. 269, 1984.
- [3] B. Häusler, F. Melzner, J. Stöcker, P. Parigger, K. Sigrütz, R. Schöning, E. Seidenschwang, F. Eberl, B. Merz, U. Pagel, E.

- Wiezorrek, and P. Genzel, "The AMPTE IRM spacecraft," *IEEE Trans. Geosci. Remote Sensing*, this issue, pp. 192-201.
- [4] S. D. Shawhan, "Magnetospheric plasma waves," in *Solar System Plasma Physics*, vol. III, L. J. Lanzerotti, C. F. Kennel, and E. H. Parker, Eds. New York: Elsevier, 1979, p. 211.
- [5] —, "Magnetospheric plasma wave research 1975-1978," *Rev. Geophys. Space Phys.*, vol. 17, p. 705, 1979.
- [6] R. R. Anderson, "Plasma waves in planetary magnetospheres," *Rev. Geophys. Space Phys.*, vol. 21, p. 474, 1983.
- [7] R. R. Anderson, C. C. Harvey, M. M. Hoppe, B. T. Tsurutani, T. E. Eastman, and J. Etcheto, "Plasma waves near the magnetopause," *J. Geophys. Res.*, vol. 87, p. 2087, 1982.
- [8] P. Rodriguez, "Magnetosheath electrostatic turbulence," *J. Geophys. Res.*, vol. 84, p. 917, 1979.
- [9] D. A. Gurnett, L. A. Frank, and R. P. Lepping, "Plasma waves in the distant magnetotail," *J. Geophys. Res.*, vol. 81, p. 6059, 1976.
- [10] R. R. Anderson, G. K. Parks, T. E. Eastman, D. A. Gurnett, and L. A. Frank, "Plasma waves associated with energetic particles streaming into the solar wind from the Earth's bow shock," *J. Geophys. Res.*, vol. 86, p. 4493, 1981.
- [11] P. Rodriguez and D. A. Gurnett, "Electrostatic and electromagnetic turbulence associated with the earth's bow shock," *J. Geophys. Res.*, vol. 80, p. 19, 1975.
- [12] D. A. Gurnett, and R. R. Anderson, "The kilometric radio emission spectrum: Relationship to auroral acceleration processes," in *Physics of Auroral Arc Formation*, S.-I. Akasofu and J. R. Kan, Eds. Geophys. Monograph Series, vol. 25. Washington, DC: Amer. Geophys. Union, 1981, p. 341.
- [13] G. Haerendel, "Plasma confinement and interaction experiments," in *Active Experiments in Space, Proc. Int. Symp.* (Alpbach, Austria, May 24-28, 1984), ESA-SP 195, p. 337.
- [14] "Mission definition for AMPTE, scientific and technical section," The Johns Hopkins University, Appl. Phys. Lab. and Max-Planck-Institut für Physik und Astrophysik, Institut für extraterrestrische Physik, report.
- [15] "Active magnetospheric particle tracer explorers (AMPTE), science requirements document," The Johns Hopkins University, Appl. Phys. Lab., report, May 1983.
- [16] G. Haerendel, B. Häusler, H. Föppl, G. Paschmann, E. Rieger, and A. Valenzuela, "An artificial Comet Experiment," in *Proc. ESO Workshop on the Need for Coordinated Ground-based Observations of Halley's Comet* (Paris, Apr. 29-30, 1982) P. Véron, M. Feston, and K. Kjær, Eds., p. 181.
- [17] G. Haerendel, A. Valenzuela, H. Föppl, E. Rieger, O. Bauer, "The Li/Ba release experiments on board the AMPTE IRM satellite," *IEEE Trans. Geosci. Remote Sensing*, this issue, pp. 253-258.
- [18] J. L. Luthey and N. D. Watson, "Report on the dynamic analysis of the Hawkeye I spacecraft," Univ. of Iowa, Dept. of Physic and Astronomy, Iowa City, May 1973.
- [19] B. Häusler, "Mechanical aspects concerning the 'Hawkeye-type' electric-field antenna system onboard the AMPTE/IRM satellite," Max-Planck-Institut für extraterrestrische Physik, Garching, Germany, report, Mar. 25, 1981.
- [20] D. A. Gurnett, F. L. Scarf, R. W. Fredricks, and E. J. Smith, "The ISEE-1 and ISEE-2 plasma wave investigation," *IEEE Trans. Geosci. Electron.*, vol. GE-16, no. 3, p. 225, July 1978.